Biointerface Research in Applied Chemistry
Open-Access Journal (ISSN: 2069-5837)

Article
Volume 13, Issue 3, 2022, 258
https://doi.org/10.33263/BRIAC133.258

Molecular Simulations of 6-Gingerol Loading on Graphene and Graphene Oxide for Drug Delivery Applications

M-Ali AL-Akhras [1], Basmah Odat [1], Venkatesha Narayanaswamy [2], Marwan Suleiman Mousa [3], Bashar Issa [2], Mutawakil Obeidat [4], Imaddin A. Al-Omari [5], Ihab M. Obaidat [6,*]

1 Bio-Medical Physics Laboratories, Department of Physical Sciences, Jordan University of Science & Technology, P.O. Box 3030, Irbid-22110, Jordan; alakmoh@just.edu.jo (M.A.A); hnoudat18@sci.just.edu.jo (B.O.);
2 Department of Medical Diagnostic Imaging, College of Health Sciences, University of Sharjah, Sharjah, P.O. Box 27272, UAE; venkateshnrn@gmail.com (V.N.);
3 Department of Physics, Faculty of Science, Mut'ah University, Jordan, AL-Karak; mmousa@mutah.edu.jo (M.S.M.);
4 Faculty of Science and Arts, Jordan University of Science and Technology, Jordan; mobeidat@just.edu.jo (M.O.);
5 Department of Physics, Sultan Qaboos University, P.O. Box 36, Muscat PC 123, Oman; ialomari@squ.edu.om (I.A.A);
6 Department of Physics, United Arab Emirates University, Al-Ain 15551, UAE; iobaidat@uaeu.ac.ae (I.M.O);
* Correspondence: iobaidat@uaeu.ac.ae (I.M.O.);

Scopus Author ID 10440642200
Received: 6.02.2022; Accepted: 27.03.2022; Published: 11.06.2022

Abstract: Loading of the anti-cancer drug 6-gingerol on graphene, graphene oxide, and Fe_3O_4 nanocarriers is investigated using Monte Carlo (MC) adsorption locator simulations in the gases phase. Molecular dynamics (MD) simulations are used in aqueous medium and neutral pH for the adsorption of 6-gingerol. In this study, the 6-gingerol loading ability of graphene oxide is studied as a function of the oxidation extent of graphene oxide (GO), and the effect of functional groups on drug loading properties is investigated. MC adsorption locator energy calculations which were done in a gaseous space, indicate that the 6-gingerol molecule prefers to be adsorbed at the less oxidized sites of the graphene oxide framework. The linear hydrophobic chain of the 6-gingerol molecule prefers to bind to the aromatic region of graphene oxide. In contrast, it has the least affinity for the Fe_3O_4 nanoparticle surface, which is indicated by the adsorption energies. The MD simulations were carried out in an aqueous medium under neutral pH. To determine the nature of the 6-gingerol attachment and release in the aqueous medium, radial distribution functions (RDF) were obtained from MD simulations. The RDF values suggest that the physical distance of separation depends on the oxidation extent of the graphene oxide. The MD presented in this study will help in fine-tuning nanocarrier synthetic methods for gingerol delivery applications.

Keywords: graphene oxide; 6-gingerol; drug loading; Monte Carlo simulations; molecular dynamics.

1. Introduction

Gingerols are a group of molecules consisting of phenolic compounds found in naturally occurring ginger which is consumed as a key spice food ingredient in south Asia [1,2]. Traditionally ginger (*Zingiber officinale*, Zingiberaceae) is an ancient herb that has been used to treat cold, cough, arthritis, digestive disorders, dyspepsia, vomiting, diarrhea, gastritis, asthma, inflammation, nervous disease, hepatotoxicity, and migraine [3–9]. The principal pharmacologically active molecule of ginger is 6-gingerol (1-[4'-hydroxy-3'-methoxyphenyl]-5-hydroxy-3-decanone), and the active section of the molecule is the aliphatic chain moiety

bearing a hydroxyl group [10,11]. The 6-gingerol has shown a good response to anti-cancer, anti-inflammatory, and antioxidant properties [12–14]. 6-Gingerol has been found to have anti-cancer properties through its effects on a range of biological pathways, including apoptosis, cell cycle regulation, cytotoxic action, and angiogenesis suppression [9,15]. As a result of its efficacy and modulation of several targets, as well as its safety for human usage, 6-gingerol and curcumin have the same scientific classification and are reported to have anti-inflammatory with many therapeutic effects; both have attracted attention as a possible therapeutic agents for the prevention and treatment of various cancer types [16–21]. Lishuang *et al*. have reported in vitro study showing that 2.5 µM of 6-gingerol has potent a cytotoxic activity to reduce 50% of cancer cell growth for large lung carcinoma cell lines (COR-L23) [22]. Sudipta *et al*. have reported that 6-gingerol inhibition pro-inflammatory cytokines such as tumor necrosis factor-alpha (TNF-α) and interleukin (IL-1β), and it could inhibit inflammation associated with osteoclast by reducing prostaglandin E2 levels [23]. So this attracted attention to 6-gingerol, making it a promising pharmaceutical drug for developing alternative chemical drugs. Unfortunately, lipophilic properties and poor pharmacokinetic characteristics of 6-gingerol limit its activity in drug therapy. For improving the bioavailability of 6-gingerol, a clinical formulation is needed through drug delivery vehicles. Recently, nanocarriers–based drug formulation for clinical applications is the best choice for increasing the drug stability, increasing water solubility, improving immobility of therapeutic drugs, and minimizing side effects in systematic human health [24–27]. The pharmaceutical industry is focused on developing a drug carrier system to deliver targeted and regulated medication release over time. This is important for designing nanocarriers for water-soluble medicinal compounds like curcumin and 6-gingerol [28,29]. It would be useful to create a drug carrier system that could overcome these restrictions and distribute drugs in a regulated and targeted manner. Graphene oxide is an excellent nanocarrier due to its properties, including excellent thermal and electrical conductivity and fast mobility of charge carrier, Graphene Oxide (GO) has oxide functional group (epoxy, hydroxyl, and carbonyl group) on its structure which makes graphene more stable and soluble in water [30,31]. The GO is studied as a nanocarrier for the biologically active materials with anti-cancer, antimicrobial, or anti-inflammatory properties such as gallic acid, caffeic acid, limonene, and nutmeg and cembra pine essential oils [32]. The studies have shown that some of these molecules have a strong affinity for GO, and they are water-insoluble, which makes the release of the drug molecules complicated. To address this issue, it is essential to optimize the physicochemical properties of the nanographene, such as oxidation extent, functional groups, and size of the GO sheets. GO sheet acts as functionalized graphene-based material to build drugs on its surface structure through π-π stacking, electrostatic (hydrophobic) interaction, hydrogen bonding, and van der Waals interaction [33,34]. The distinguishing properties of the 2D GO sheet make it the best biocompatibility nanocarrier for drug loading and delivery applications in cancer therapy and bio-imaging [35]. On the other hand, biocompatible material such as polyethylene glycol (PEG) can be used with nanocarrier for preserving GO from the immune system [36,37]. In addition, PEG has hydrophilic properties that can improve water solubility and stability of nanocarrier drug delivery formulation. GO with Fe_3O_4 nanocomposites are extensively studied for biomedical applications like MRI, drug delivery, and magnetic hyperthermia [38,39]. It is essential to understand the drug loading onto the surface of the Fe_3O_4 nanoparticles for targeted drug delivery. Understanding the mechanisms involved in the adsorption and release of the drug molecules like gingerol, curcumin, and doxorubicin is important. The ferrite nanoparticles are usually functionalized

with biocompatible polymers like polyethylene glycol and chitosan [40]. In this study, we use molecular simulation to tune synthetic methods of nanocarriers for 6-gingerol delivery applications and estimate of 6-gingerol loading capacity of Graphene, GO with different oxidation extent. Also, 6-gingerol loading capacity of GO and Fe3O4 nanoparticles is obtained using Monte Carlo adsorption locator simulation. The adsorption locator helps determine the basic interaction responsible for the adsorption of 6-gingerol on the GO sheet. Adsorption locator energy calculations were used to determine adsorption preference at the preferred site of GO. Radial distribution function calculations are obtained from molecular dynamic (MD) trajectories and the equilibrium distance of separation 6-gingerol from the GO sheet. This study aims to design and simulate new synthetic methods of nanocarrier such as Graphene and Graphene Oxide for 6-gingerol delivery applications using MD and Monte Carlo simulation.

2. Computational Method

The Models of Gingerol, Graphene, GO1, and GO2 were created in BIOVIA Materials Studio (V7.0). To create the GO sheets, the graphene sheet surface was randomly decorated with hydroxyl and epoxide groups. Graphene oxide with two different oxidation densities was created. The highly oxidized GO is denoted as GO2, and the least oxidized sheet as GO1. The energy and geometry of the Gingerol, Graphene, GO1, and GO2 were optimized using the DREIDING force field. DREIDING is a generic force field that is used to predict the structures and dynamics of organic, biological, and inorganic functional-group molecules. DREIDING follows the universal force constants and geometry parameters based on simple hybridization considerations rather than individual force constants and geometric factors dependent on the specific atom combinations involved in the bond, angle, or torsion terms. DREIDING force field will describe interactions involving a hydrogen bonding atom due to electronegative atoms [41]. The structures of gingerol, graphene, GO1, and GO2 are shown in Figure 1.

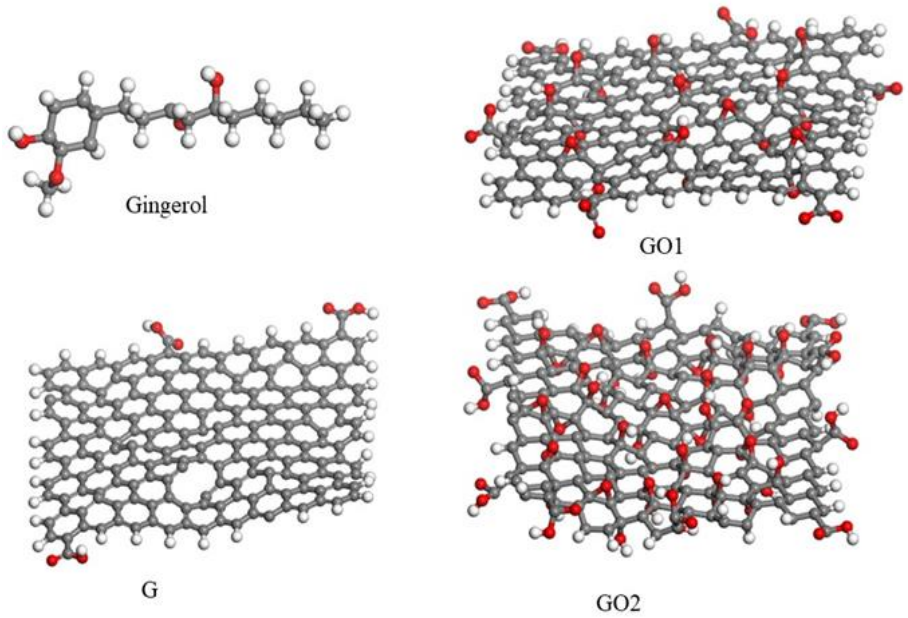

Figure 1. Geometry and energy-optimized gingerol, graphene, GO1, and GO2 (Gray-C atoms, White-H atoms, Red-O atoms).

2.1. Monte Carlo adsorption locator simulations.

Adsorption locator studies were designed to examine the gingerol interaction with graphene GO1, and GO2 surfaces. Studies would seek to compare the energy-minimized binding configurations as well as adsorption energies. Molecular mechanics tools were used to investigate the Graphene/ GO1/GO2-Gingerol systems.

The adsorption Locator module in Materials Studio was used to predict the adsorption of the gingerol molecules on GO1,2 and graphene surfaces. The adsorption locator helps find the most stable adsorption sites for the range of materials. Energy and geometry optimized gingerol molecules have been simulated as adsorbate on graphene/GO1,2 substrate surfaces to find the lowest energy adsorption configurations and investigate gingerol molecules' preferential adsorption sites. The Monte Carlo method is used to calculate the adsorption configurations and binding energy of drug molecules [42,43].

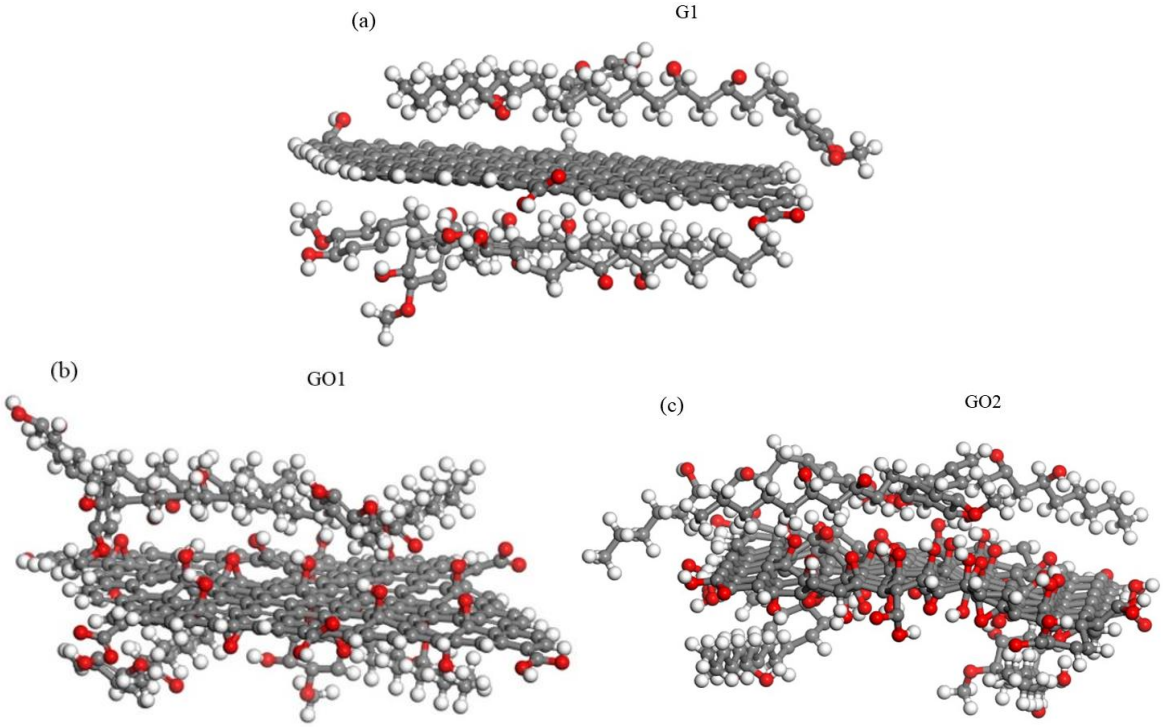

Figure 2. One of the configurations of (**a**) Gingerol/graphene, (**b**) Gingerol/GO1, and (**c**) Gingerol/GO2 systems obtained by adsorption locator using the Monte Carlo Method. (Gray-C atoms, White-H atoms, Red-O atoms).

This computational work identified possible adsorption configurations by carrying out Monte Carlo searches of configurational adsorption of 6-Gingerol/G/GO1,2 and Fe_3O_4 systems for minimum energy configurations from which the average values of the adsorption energies were calculated. One of the configurations for each Gingerol/graphene/GO1,2 system is shown in Figure 2. The corresponding adsorption energies of the minimum adsorption energy configurations are listed in Table 1.

Table 1. Energies obtained from an Adsorption Locator calculation. The energy of the stable GO1,2-Gingerol and Graphene-Gingerol configurations.

Structures	Adsorption energy (kcal/mol)	Rigid adsorption energy (kcal/mol)	Deformation energy (kcal/mol)
Graphene-Gingerol	-133.78	-142.68	8.89
GO1-Gingerol	-110.22	-117.69	7.47
GO2-Gingerol	-109.38	-115.38	5.96
Fe_3O_4-Gingerol	-59.20	-61.90	2.70

These MC simulations were obtained in the gas phase for the well-separated molecules. The trend of adsorption energies of the ensembles calculated was compared with the ones obtained from the MD simulations.

MC simulation can reasonably predict the most favorable configuration for the 6-gingerol molecule adsorption on the graphene framework. The 6-gingerol molecule is placed near the graphene framework, and optimization is run under quench molecular dynamics simulations. The adsorption energy consists of van der Waals energy and intramolecular energy using MC simulations are shown in Figure 3.

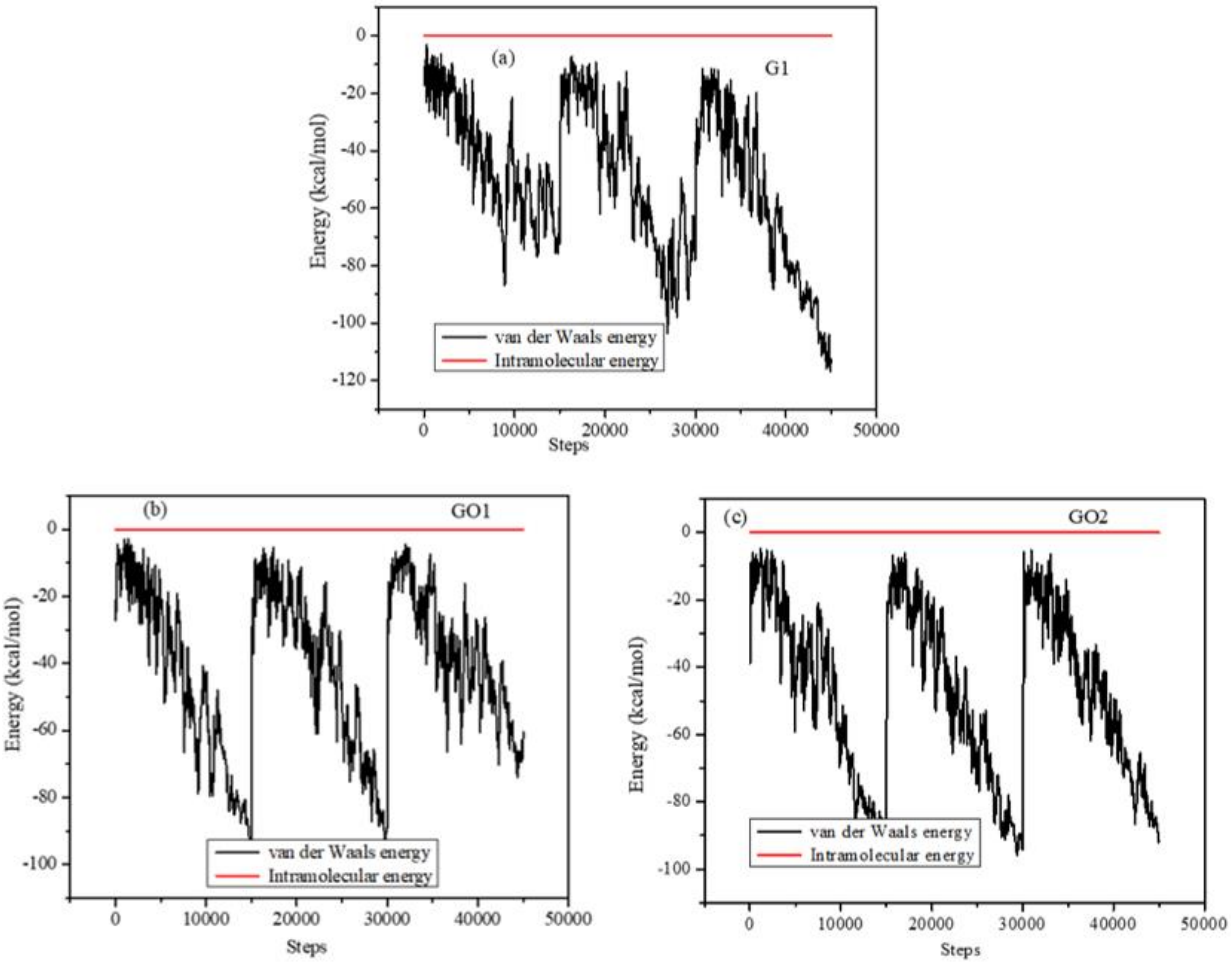

Figure 3. Average van der Waals and intramolecular energies of the (**a**) 6-gingerol/Graphene, (**b**) 6-gingerol/GO1, and (**c**) 6-gingerol/GO2.

In calculating adsorption locators, the metropolis Monte Carlo approach involves four steps for the 6-gingerol adsorption on the graphene surface. The molecules tend to form a stable conformer through rotation, translation, and regrowth to form the canonical ensemble. The adsorption energy determines the affinity of the 6-gingerol molecule to adsorb on the G/GO1,2/Fe_3O_4 surface. In the MC calculations, substrate energy (G/GO1,2/Fe_3O_4) is taken as zero. The adsorption energy (in $kJmol^{-1}$) reports the energy released when the relaxed 6-gingerol is adsorbed on the G/GO1,2/Fe_3O_4 surface. The adsorption energy is calculated from the sum of the rigid adsorption energy and the deformation energy for the 6-gingerol molecule. The rigid adsorption energy (in $kJmol^{-1}$) reports the energy released when the unrelaxed 6-gingerol molecules (i.e., before the geometry optimization step) are adsorbed on the substrate. The deformation energy (in $kJmol^{-1}$) reports the energy gained when the adsorbed 6-gingerol molecule is relaxed on the substrate surface. From the adsorption energy values, the

energetically favored adsorption sites for 6-gingerol are the less oxidized GO sites. The adsorption density (high probability for adsorption) is shown in Figure 4, in which there is no peak, indicating that the adsorption is favored over the range of energies.

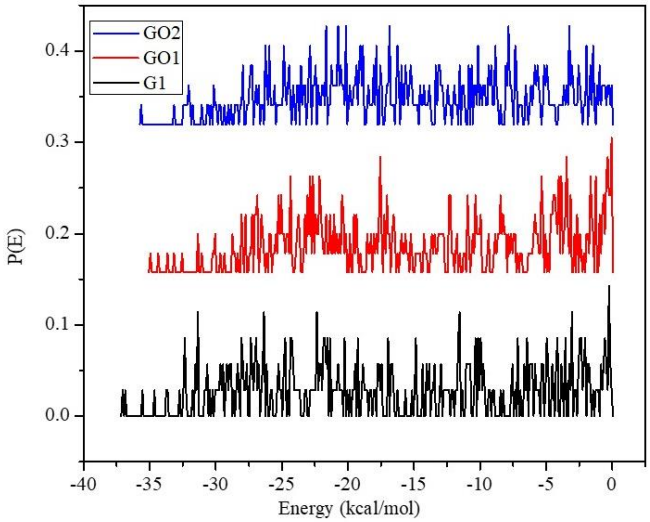

Figure 4. Adsorption energy distribution of the adsorbate 6-gingerol on Graphene, GO1, and GO2 surface.

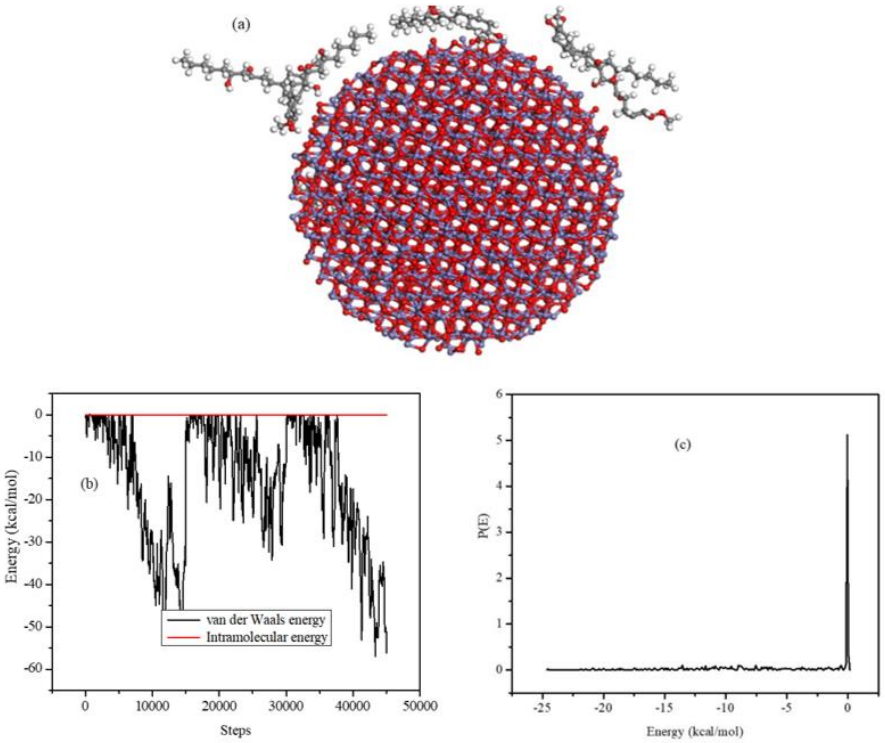

Figure 5. One of the configurations of (**a**) 6-gingerol/Fe_3O_4 nanoparticle system, (**b**) Average van der Waals and intramolecular interaction energies of the 6-gingerol/Fe_3O_4, and (**c**) Adsorption energy distribution of the adsorbate 6-gingerol on Fe_3O_4.

The MC adsorption locator calculations for the 6-gingerol loading on the Fe_3O_4 nanoparticles are obtained with the similar force field and parameters used for the graphene oxide. The orientation of the 6-gingerol molecule on the nanoparticle surface is shown in Figure 5(a). The energy distribution for the adsorption process is given from the probability density plot shown in Figure 5(c). The peak at energy -2 kcal/mol indicates that the high number of 6-gingerol molecules are adsorbed at this energy. The adsorption energies trends shown in table

1 show that the 6-gingerol has the least affinity for the Fe_3O_4 surface compared to the graphene framework.

2.2. Molecular dynamics.

MD simulations of 6-gingerol–GO1/GO2 in an aqueous solution were carried out using a material studio. The energy and geometry of the GO1,2 sheet and 6-gingerol molecules are minimized using the DREIDING force field and eventually solvated in a cubic box with 1000 water molecules. A nose thermostat was used to control the system at a constant temperature, and pressure was maintained constant using Berendsen-Barostat [44]. Periodic boundary conditions were applied, and simulations were conducted using the NPT ensemble (constant-temperature, constant-pressure ensemble) with a constant pressure of 1 bar and constant temperature of 298 K. Van der Waals interactions were treated with a cutoff distance of 12.5 Å and long-range electrostatic interactions were treated using particle-particle/ particle-mesh (PPPM) method.

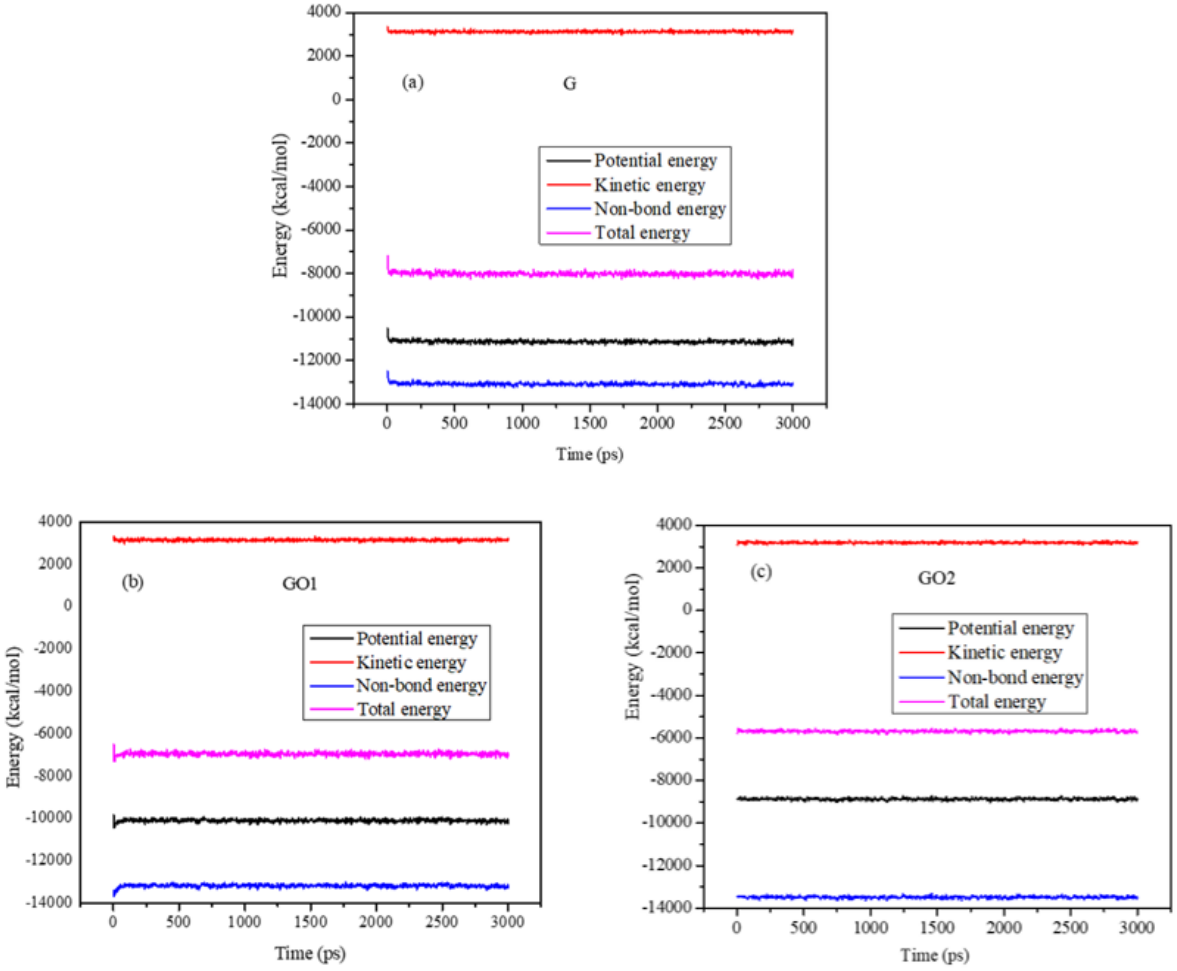

Figure 6. Total energy fluctuations during Molecular dynamics simulations for 3000 ps of the (**a**) 6-gingerol/Graphene, (**b**) 6-gingerol/GO1, and (**c**) 6-gingerol/GO2.

The simulations were conducted for a time period of 3 ns, and the trajectories, velocities, and forces corresponding to all molecules in the system were saved every 5 ps. The simulation time of 3 ns provides the best optimization between computational time and the MD results obtained. Initial geometries of the simulation box were generated using an amorphous cell module by ramping the density from 0.6 to 1 g/cm3 in Material Studio. The energy and geometry of the solvated box are minimized using the DREIDING force field and forcite

module. Energy fluctuation during the MD simulations is provided in Figure 6 (a, b, c). The total energy of the equilibrated canonical ensemble 6-gingerol-G/GO1,2 is -7944.3, -7015.3, and -5703.7 kcal/mol for the 6-gingerol adsorption on the G, GO1, and GO2 sheets, respectively. The negative energies of the equilibrated systems under neutral pH indicate that the 6-gingerol forms a stable complex with the graphene surface and a high dependency on oxidation.

Possible interactions between Graphene, GO1,2, and 6-gingerol molecules include van der Waals, electrostatic, hydrophobic (interaction between water and aromatic rings of graphene framework), π-π bonding, and hydrogen bonding with the hydroxyl groups of GO. Functional groups (carbonyl, hydroxyl, and Carboxyl) of GO enhance the adsorption of 6-gingerol through electrostatic interactions. GO possess C=C double bond framework, which helps in the π-π bonding interaction. Equilibrium configurations obtained through MD simulations and adsorption locator confirm that the predominant interaction is π-π electron coupling for the adsorption of 6-gingerol on graphene and GO sheets.

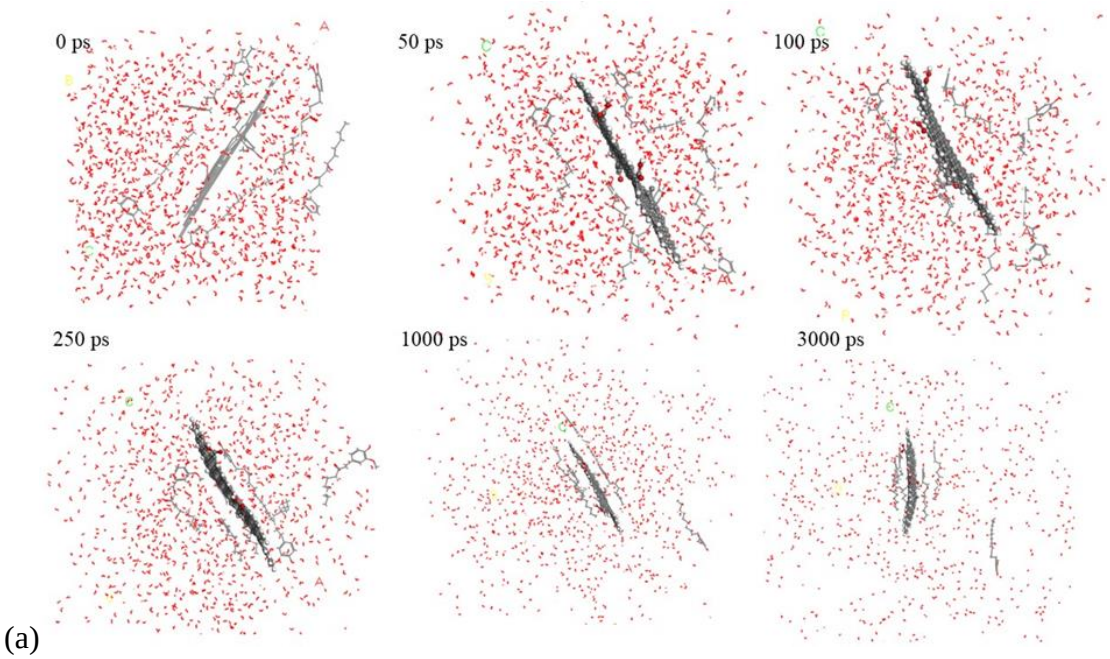

(a)

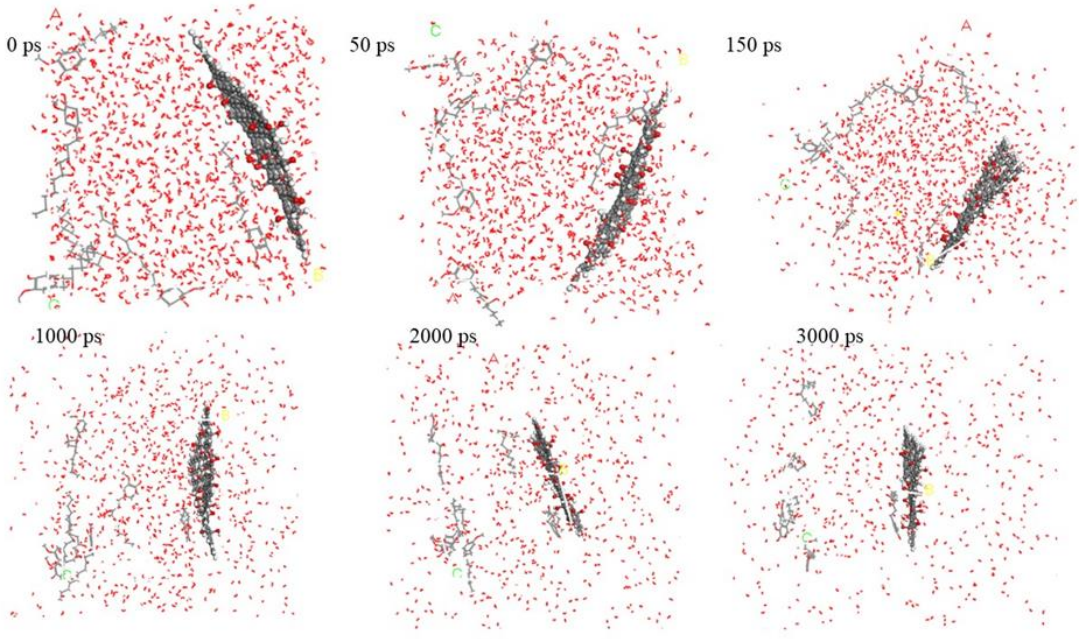

(b)

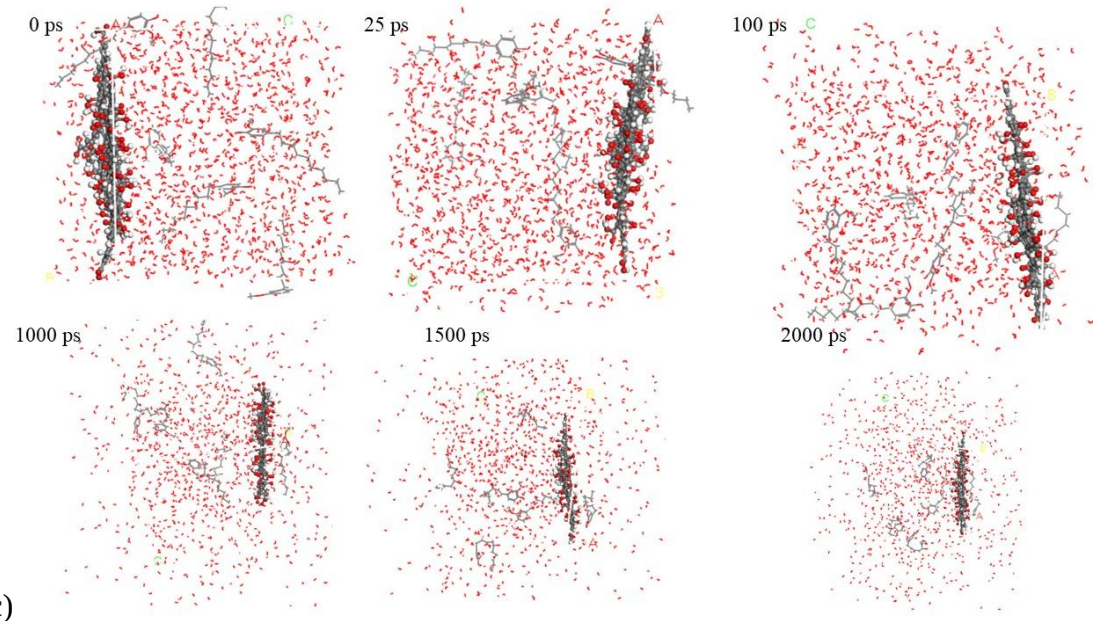

(c)

Figure 7. (**a**) Molecular dynamics simulations snapshots of 6-gingerol/Graphene. **(b)** Molecular dynamics simulations snapshots of 6-gingerol/GO1. **(c)** Molecular dynamics simulations snapshots of 6-gingerol/GO2.

The equilibrium distance between the 6-gingerol molecule and G/GO sheet is obtained by calculating the Radial Distribution Function (RDF). The RDF defines the probability of finding a 6-gingerol molecule at a distance r from the G/GO surface [45]. The average distance of the gingerol molecules from the substrate surface is shown in Figure 8.

$$g(r) = \frac{n(r)}{2\pi r \text{Þ}}$$

r - the distance between 6-gingerol molecules from surface atoms of GO;

n(r) - time-averaged number of 6-gingerol molecules in r ± Δr;

Þ - number density of the system.

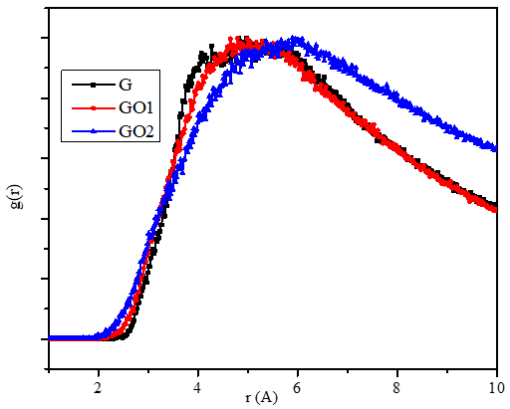

Figure 8. Radial distribution functions between 6-gingerol and Graphene/GO1,2 obtained from the MD calculations.

The 6-gingerol molecule is at 4.80 A from the graphene and GO1 sheet, whereas its distance of separation from the GO2 sheet is 5.89 A. This physical distance of interaction is attributed to the functional groups present on the GO2 sheet. This indicated the non-oxidized part of the graphene oxide could serve as a preferred site for the loading of water-insoluble drug molecules through the π-π bonding, covalent, hydrogen bonding, π-π bonding, hydrophobic, electrostatic, and van der Waals forces at the surfaces.

3. Conclusions

Using a Monte Carlo adsorption locator and MD simulations, the drug loading capacity of 6-gingerol on graphene and graphene oxide sheets with varying degrees of oxidation was determined. The drug loading capacity of the graphene oxide sheet is shown by MC loading to be dependent on the extent of oxidation. The pristine graphene can adsorb more drugs, whereas the highly oxidized graphene can adsorb less. The Fe_3O_4 nanosurface has less 6-gingerol loading capacity than the GO; optimizing the properties of GO-ferrite nanocomposite will assist in designing the high drug loading and releasing agents. The adsorption energies obtained for graphene, GO/6-gingerol configurations also show that 6-gingerol loading is high for pristine graphene but low for highly oxidized graphene oxide sheet GO2. 6-gingerol shows a high affinity for the graphene framework compared to the Fe_3O_4 surface. Molecular dynamic simulations using the NPT ensemble at neutral pH also show that 6-gingerol loading is lower for the highly oxidized GO sheet. Even though the loading capacity of GO1 and GO2 differ, the equilibrium distance of separation of 6-gingerol on GO1 and GO2 is comparable. The equilibrium configurations obtained after 3000 ps simulation time show that only a few molecules were adsorbed on the GO2 sheet, whereas the GO2 sheet has a higher number of 6-gingerol molecules. The simulation studies presented here give insight to the required properties of the nanocarrier synthesis for 6-gingerol loading and releasing agents.

Funding

The authors would like to thank the Jordan University of Science and Technology; Scientific Research's Deanship for supporting this research under Grant Number 69/2022

Conflicts of Interest

The authors declare no conflict of interest; the funders had no role in the study's design, in the collection, analyses, or interpretation of data, in the writing of the manuscript, or in the decision to publish the results.

References

1. Unuofin, J.O.; Masuku, N.P.; Paimo, O.K.; Lebelo, S.L. Ginger from Farmyard to Town: Nutritional and Pharmacological Applications. *Frontiers in Pharmacology* **2021**, *12*, http://doi.org/10.3389/fphar.2021.779352.
2. Ajayi, O.B.; Akomolafe, S.F.; Akinyemi, F.T. Food Value of Two Varieties of Ginger (Zingiber Officinale) Commonly Consumed in Nigeria. *ISRN Nutrition* **2013**, *2013*, e359727, http://doi.org/10.5402/2013/359727.
3. Mohd Yusof, Y.A. Gingerol and Its Role in Chronic Diseases. *Adv Exp Med Biol* **2016**, *929*, 177–207, https://doi.org/10.1007/978-3-319-41342-6_8.
4. Zivarpour, P.; Nikkhah, E.; Maleki Dana, P.; Asemi, Z.; Hallajzadeh, J. Molecular and Biological Functions of Gingerol as a Natural Effective Therapeutic Drug for Cervical Cancer. *J Ovarian Res* **2021**, *14*, 43, https://doi.org/10.1186/s13048-021-00789-x.
5. Manjunathan, T.; Guru, A.; Arokiaraj, J.; Gopinath, P. 6-Gingerol and Semisynthetic 6-Gingerdione Counteract Oxidative Stress Induced by ROS in Zebrafish. *Chemistry & Biodiversity* **2021**, *18*, e2100650, https://doi.org/10.1002/cbdv.202100650.
6. Wang, S.; Zhang, C.; Yang, G.; Yang, Y. Biological Properties of 6-Gingerol: A Brief Review. *Nat Prod Commun* **2014**, *9*, 1027–1030, https://doi.org/10.1177/1934578X1400900736.
7. Fitzpatrick, L.R.; Woldemariam, T. 5.16 - Small-Molecule Drugs for the Treatment of Inflammatory Bowel Disease. In *Comprehensive Medicinal Chemistry III*; Chackalamannil, S.; Rotella, D.; Ward, S.E. Elsevier: Oxford, **2017**; pp. 495–510.

8. Liu, H.; Yang, H.; Zhao, T.; Lin, C.; Li, Y.; Zhang, X.; Ye, Y.; Liao, J. Combined Metabolome and Transcriptome Analyses of Young, Mature, and Old Rhizome Tissues of Zingiber Officinale Roscoe. *Frontiers in Genetics* **2021**, *12*, http://doi.org/10.3389/fgene.2021.795201.
9. Manatunga, D.C.; de Silva, R.M.; de Silva, K.M.N.; Wijeratne, D.T.; Malavige, G.N.; Williams, G. Fabrication of 6-Gingerol, Doxorubicin and Alginate Hydroxyapatite into a Bio-Compatible Formulation: Enhanced Anti-Proliferative Effect on Breast and Liver Cancer Cells. *Chemistry Central Journal* **2018**, *12*, 119, https://doi.org/10.1186/s13065-018-0482-6.
10. Levita, J.; Syafitri, D.M.; Supu, R.D.; Mutakin, M.; Megantara, S.; Febrianti, M.; Diantini, A. Pharmacokinetics of 10-Gingerol and 6-Shogaol in the Plasma of Healthy Subjects Treated with Red Ginger (Zingiber Officinale Var. Rubrum) Suspension. *Biomed Rep* **2018**, *9*, 474–482, https://doi.org/10.3892/br.2018.1163.
11. Qiu, J.-X.; Zhou, Z.-W.; He, Z.-X.; Zhang, X.; Zhou, S.-F.; Zhu, S. Estimation of the Binding Modes with Important Human Cytochrome P450 Enzymes, Drug Interaction Potential, Pharmacokinetics, and Hepatotoxicity of Ginger Components Using Molecular Docking, Computational, and Pharmacokinetic Modeling Studies. *DDDT* **2015**, *9*, 841–866, https://doi.org/10.2147/DDDT.S74669.
12. Young, H.-Y.; Luo, Y.-L.; Cheng, H.-Y.; Hsieh, W.-C.; Liao, J.-C.; Peng, W.-H. Analgesic and Anti-Inflammatory Activities of [6]-Gingerol. *Journal of Ethnopharmacology* **2005**, *96*, 207–210, https://doi.org/10.1016/j.jep.2004.09.009.
13. Sp, N.; Kang, D.Y.; Lee, J.-M.; Bae, S.W.; Jang, K.-J. Potential Antitumor Effects of 6-Gingerol in P53-Dependent Mitochondrial Apoptosis and Inhibition of Tumor Sphere Formation in Breast Cancer Cells. *International Journal of Molecular Sciences* **2021**, *22*, 4660, https://doi.org/10.3390/ijms22094660.
14. Wang, C.-C.; Chen, L.-G.; Lee, L.-T.; Yang, L.-L. Effects of 6-Gingerol, an Antioxidant from Ginger, on Inducing Apoptosis in Human Leukemic HL-60 Cells. *In Vivo* **2003**, *17*, 641–645.
15. Poltronieri, J.; Becceneri, A.B.; Fuzer, A.M.; Filho, J.C.C.; Martin, A.C.B.M.; Vieira, P.C.; Pouliot, N.; Cominetti, M.R. [6]-Gingerol as a Cancer Chemopreventive Agent: A Review of Its Activity on Different Steps of the Metastatic Process. *Mini Rev Med Chem* **2014**, *14*, 313–321, https://doi.org/10.2174/1389557514666140219095510.
16. Adahoun, M.A.; Al-Akhras, M.-A.H.; Jaafar, M.S.; Bououdina, M. Enhanced Anti-Cancer and Antimicrobial Activities of Curcumin Nanoparticles. *Artif Cells Nanomed Biotechnol* **2017**, *45*, 98–107, https://doi.org/10.3109/21691401.2015.1129628.
17. Aldahoun, M.A.; Jaafar, M.S.; Al-Akhras, M.-A.H.; Bououdina, M. Enhanced Nanocurcumin Toxicity against (PC3) Tumor and Microbial by Using Magnetic Field in Vitro. *Artif Cells Nanomed Biotechnol* **2017**, *45*, 843–853, https://doi.org/10.1080/21691401.2016.1178137.
18. Narayanaswamy, V.; Alaabed, S.; Issa, B.; AL-Akhras, M.-A.; Obaidat, I.M. Molecular Simulation of Curcumin Loading on Graphene and Graphene Oxide for Drug Delivery Applications. *Current Chemistry Letters* **2021**, 161–168, https://doi.org/10.5267/j.ccl.2020.12.003.
19. Bajpai, S.K.; Chand, N.; Ahuja, S. Investigation of Curcumin Release from Chitosan/Cellulose Micro Crystals (CMC) Antimicrobial Films. *International Journal of Biological Macromolecules* **2015**, *79*, 440–448, https://doi.org/10.1016/j.ijbiomac.2015.05.012.
20. Soumya, T.; Lakshmipriya, T.; Klika, K.D.; Jayasree, P.R.; Manish Kumar, P.R. Anticancer Potential of Rhizome Extract and a Labdane Diterpenoid from Curcuma Mutabilis Plant Endemic to Western Ghats of India. *Sci Rep* **2021**, *11*, 552, https://doi.org/10.1038/s41598-020-79414-8.
21. Setyawati, A.; Komariah; Pujiasmanto, B.; Fatawi, A.; Batubara, I. Secondary Metabolites of Turmeric and Ginger on Various Altitudes and Soil Characteristics. *IOP Conf. Ser.: Earth Environ. Sci.* **2021**, *724*, 012020, https://doi.org/10.1088/1755-1315/724/1/012020.
22. Lv, L.; Chen, H.; Soroka, D.; Chen, X.; Leung, T.; Sang, S. 6-Gingerdiols as the Major Metabolites of 6-Gingerol in Cancer Cells and in Mice and Their Cytotoxic Effects on Human Cancer Cells. *J Agric Food Chem* **2012**, *60*, 11372–11377, https://doi.org/10.1021/jf303879b.
23. Tripathi, S.; Maier, K.G.; Bruch, D.; Kittur, D.S. Effect of 6-Gingerol on pro-Inflammatory Cytokine Production and Costimulatory Molecule Expression in Murine Peritoneal Macrophages. *J Surg Res* **2007**, *138*, 209–213, https://doi.org/10.1016/j.jss.2006.07.051.
24. Yao, Y.; Zhou, Y.; Liu, L.; Xu, Y.; Chen, Q.; Wang, Y.; Wu, S.; Deng, Y.; Zhang, J.; Shao, A. Nanoparticle-Based Drug Delivery in Cancer Therapy and Its Role in Overcoming Drug Resistance. **2020**, *7*, https://doi.org/10.3389/fmolb.2020.00193.

25. Mitchell, M.J.; Billingsley, M.M.; Haley, R.M.; Wechsler, M.E.; Peppas, N.A.; Langer, R. Engineering Precision Nanoparticles for Drug Delivery. *Nat Rev Drug Discov* **2021**, *20*, 101–124, https://doi.org/10.1038/s41573-020-0090-8.
26. Rambaran, T.F.; Nordström, A. Medical and Pharmacokinetic Effects of Nanopolyphenols: A Systematic Review of Clinical Trials. *Food Frontiers* **2021**, *2*, 140–152, https://doi.org/10.1002/fft2.72.
27. Firouzjaei, L.G.; Mohammadi, M.; Darzi, G.N.; Nikzad, M.; Kazemi, S. Synthesis, Characterization, and in-Vitro Evaluation of Piperine-Loaded Silica/Hydroxyapatite Mesoporous Nanoparticles. *Chem. Pap.* **2021**, *75*, 6465–6475, https://doi.org/10.1007/s11696-021-01813-6.
28. Hu, Y.; He, Y.; Ji, J.; Zheng, S.; Cheng, Y. <p>Tumor Targeted Curcumin Delivery by Folate-Modified MPEG-PCL Self-Assembly Micelles for Colorectal Cancer Therapy</P>. *IJN* **2020**, *15*, 1239–1252, https://doi.org/10.2147/IJN.S232777.
29. Singh, R.P.; Gangadharappa, H.V.; Mruthunjaya, K. Phytosome Complexed with Chitosan for Gingerol Delivery in the Treatment of Respiratory Infection: In Vitro and in Vivo Evaluation. *Eur J Pharm Sci* **2018**, *122*, 214–229, https://doi.org/10.1016/j.ejps.2018.06.028.
30. Ghosal, K.; Sarkar, K. Biomedical Applications of Graphene Nanomaterials and Beyond. *ACS Biomater. Sci. Eng.* **2018**, *4*, 2653–2703, https://doi.org/10.1021/acsbiomaterials.8b00376.
31. Chung, C.; Kim, Y.-K.; Shin, D.; Ryoo, S.-R.; Hong, B.H.; Min, D.-H. Biomedical Applications of Graphene and Graphene Oxide. *Acc. Chem. Res.* **2013**, *46*, 2211–2224, https://doi.org/10.1021/ar300159f.
32. Croitoru, A.; Oprea, O.; Nicoara, A.; Trusca, R.; Radu, M.; Neacsu, I.; Ficai, D.; Ficai, A.; Andronescu, E. Multifunctional Platforms Based on Graphene Oxide and Natural Products. *Medicina (Kaunas)* **2019**, *55*, 230, https://doi.org/10.3390/medicina55060230.
33. Mahdavi, M.; Rahmani, F.; Nouranian, S. Molecular Simulation of PH-Dependent Diffusion, Loading, and Release of Doxorubicin in Graphene and Graphene Oxide Drug Delivery Systems. *J. Mater. Chem. B* **2016**, *4*, 7441–7451, https://doi.org/10.1039/C6TB00746E.
34. Rahmani, F.; Nouranian, S.; Mahdavi, M.; Al-Ostaz, A. Molecular Simulation Insights on the in Vacuo Adsorption of Amino Acids on Graphene Oxide Surfaces with Varying Surface Oxygen Densities. *J Nanopart Res* **2016**, *18*, 320, https://doi.org/10.1007/s11051-016-3631-7.
35. Gonçalves, G.; Vila, M.; Portolés, M.-T.; Vallet-Regi, M.; Gracio, J.; Marques, P.A.A.P. Nano-Graphene Oxide: A Potential Multifunctional Platform for Cancer Therapy. *Advanced Healthcare Materials* **2013**, *2*, 1072–1090, https://doi.org/10.1002/adhm.201300023.
36. Jihad, M.A.; Noori, F.T.M.; Jabir, M.S.; Albukhaty, S.; AlMalki, F.A.; Alyamani, A.A. Polyethylene Glycol Functionalized Graphene Oxide Nanoparticles Loaded with Nigella Sativa Extract: A Smart Antibacterial Therapeutic Drug Delivery System. *Molecules* **2021**, *26*, 3067, https://doi.org/10.3390/molecules26113067.
37. Sattari, S.; Adeli, M.; Beyranvand, S.; Nemati, M. Functionalized Graphene Platforms for Anticancer Drug Delivery. *Int J Nanomedicine* **2021**, *16*, 5955–5980, https://doi.org/10.2147/IJN.S249712.
38. Cardoso, V.F.; Francesko, A.; Ribeiro, C.; Bañobre-López, M.; Martins, P.; Lanceros-Mendez, S. Advances in Magnetic Nanoparticles for Biomedical Applications. *Advanced Healthcare Materials* **2018**, *7*, 1700845, https://doi.org/10.1002/adhm.201700845.
39. Laurent, S.; Bridot, J.-L.; Elst, L.V.; Muller, R.N. Magnetic Iron Oxide Nanoparticles for Biomedical Applications. *Future Med Chem* **2010**, *2*, 427–449, https://doi.org/10.4155/fmc.09.164.
40. Ignat, M.; Samoila, P.; Cojocaru, C.; Sacarescu, L.; Harabagiu, V. Novel Synthesis Route for Chitosan-Coated Zinc Ferrite Nanoparticles as Potential Sorbents for Wastewater Treatment. *Chemical Engineering Communications* **2016**, *203*, 1591–1599, https://doi.org/10.1080/00986445.2016.1185711.
41. Sasaki, K.; Yamashita, T. Modification and Validation of the DREIDING Force Field for Molecular Liquid Simulations (DREIDING-UT). *J. Chem. Inf. Model.* **2021**, *61*, 1172–1179, https://doi.org/10.1021/acs.jcim.0c01169.
42. Akkermans, R.L.C.; Spenley, N.A.; Robertson, S.H. Monte Carlo Methods in Materials Studio. *Molecular Simulation* **2013**, *39*, 1153–1164, https://doi.org/10.1080/08927022.2013.843775.
43. Pelalak, R.; Soltani, R.; Heidari, Z.; Malekshah, R.E.; Aallaei, M.; Marjani, A.; Rezakazemi, M.; Shirazian, S. Synthesis, Molecular Dynamics Simulation and Adsorption Study of Different Pollutants on Functionalized Mesosilica. *Sci Rep* **2021**, *11*, 1967, https://doi.org/10.1038/s41598-020-80566-w.
44. Lin, Y.; Pan, D.; Li, J.; Zhang, L.; Shao, X. Application of Berendsen Barostat in Dissipative Particle Dynamics for Nonequilibrium Dynamic Simulation. *J. Chem. Phys.* **2017**, *146*, 124108, https://doi.org/10.1063/1.4978807.

45. Levine, B.G.; Stone, J.E.; Kohlmeyer, A. Fast Analysis of Molecular Dynamics Trajectories with Graphics Processing Units-Radial Distribution Function Histogramming. *J Comput Phys* **2011**, *230*, 3556–3569, https://doi.org/10.1016/j.jcp.2011.01.048.